

The vulnerability of the European air traffic network to spatial hazards

Sean M. Wilkinson · Sarah Dunn · Shu Ma

Received: 8 April 2011 / Accepted: 24 June 2011 / Published online: 19 August 2011
© The Author(s) 2011. This article is published with open access at Springerlink.com

Abstract The 2010 eruption of the Eyjafjallajökull volcano had a devastating effect on the European air traffic network, preventing air travel throughout most of Europe for 6 days (Oroian in *ProEnvironment* 3:5–8, 2010). The severity of the disruption was surprising as previous research suggests that this type of network should be tolerant to random hazard (Albert et al. in *Nature* 406(6794):378–382, 2000; Strogatz in *Nature* 410(6825):268–276, 2001). The source of this hazard tolerance lies in the degree distribution of the network which, for many real-world networks, has been shown to follow a power law (Albert et al. in *Nature* 401(6749):130–131, 1999; Albert et al. in *Nature* 406(6794):378–382, 2000). In this paper, we demonstrate that the ash cloud was unexpectedly disruptive because it was spatially coherent rather than uniformly random. We analyse the spatial dependence in air traffic networks and demonstrate how the combination of their geographical distribution and their network architectures jeopardises their inherent hazard tolerance.

Keywords Network reliability · Scale-free networks · Spatial hazard · Airline networks · Hazard tolerance · Exponential networks

1 Introduction

Complex networks can be found in all aspects of modern society. Many of these complex networks, including the Internet and World Wide Web, have been shown to be scale-free (Barabasi and Albert 1999; Albert et al. 2000). Scale-free networks are networks whose degree distribution (defined as the cumulative probability distribution of the number of connections that each node has to other nodes, see Fig. 1a, b for further explanation) follows a power law and therefore comprises a small number of high-degree nodes and a large number of smaller-degree nodes. They have been shown to be resilient to random hazard and vulnerable to targeted attack as a random hazard has a small chance of removing a high-degree node, whereas an informed and pernicious agent will target the

S. M. Wilkinson (✉) · S. Dunn · S. Ma
School of Civil Engineering and Geosciences, Newcastle University, Newcastle upon Tyne, UK
e-mail: s.m.wilkinson@ncl.ac.uk

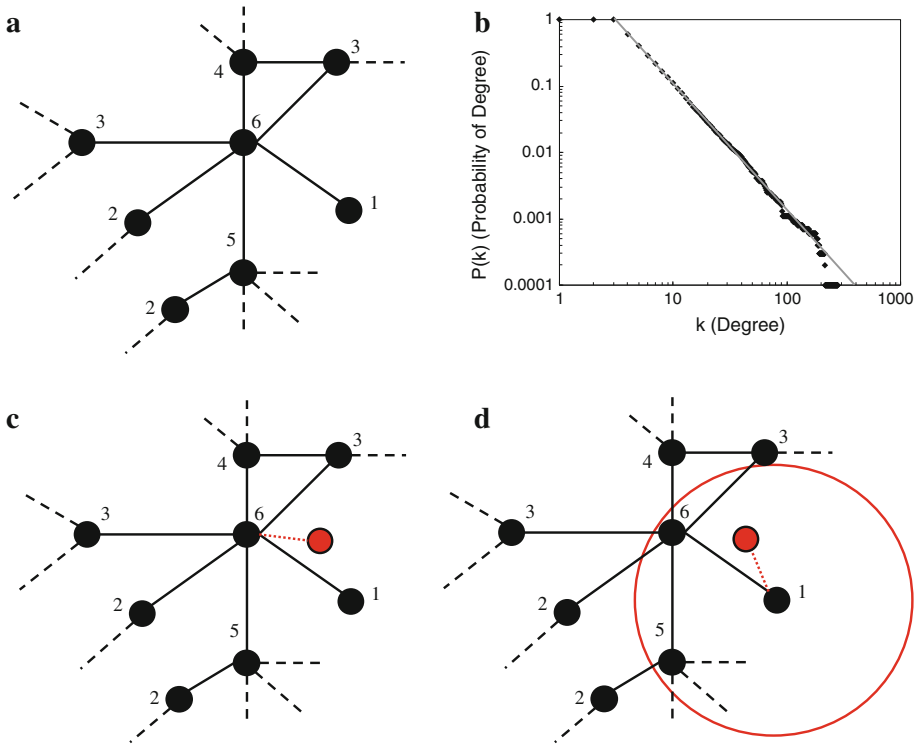


Fig. 1 The calculation of degree distribution is made by obtaining the degree of each node. The degree of a node, k , is the number of links attached to this node from other nodes, for example, if a node has 3 links attached to it, then it has a degree of 3. **a** shows a small sample from a scale-free network, created using Network Workbench, and shows the degree of each node (the *dashed lines* indicate links to other nodes in the network that have been removed from this figure for clarity). The degree distribution of the network, $P(k)$, gives the cumulative probability that a selected node has k or greater links. $P(k)$ is calculated by summing the number of nodes with $k = 1, 2, \dots$ links divided by the total number of nodes. It is this distribution that allows for the distinction between different classes of network and also defines the inherent hazard tolerance of the network (Barabasi and Oltvai 2004). The degree distribution for the scale-free network (partly shown in **a**) is shown in **b**. Preferential attachment based on degree and based on both proximity and degree is indicated in **c** and **d**, respectively. In **c**, a new node (in *red*) is introduced into the network, and using the algorithm of Barabasi and Albert (1999) would be most likely to attach itself to the high-degree node; however, considering proximity as well as degree alters the probability because the spatial domain of the low-degree node (in the *centre* of the *red circle*) includes the high-degree node and therefore inflates its probability of attachment (desirability)

highest-degree node resulting in a disproportionately severe impact to the network (Albert et al. 2000). Those physical networks that have been shown to be scale-free (for example, the Internet and the World Wide Web) require little physical space; the routers and servers, which comprise the Internet, each require only a room, or even a small space within a room. Even the largest hubs require little physical space and little or no planning permission. The World Wide Web requires even less space. Web pages and the hyperlinks that connect them are virtual entities whose physical size amounts to only a few nanometres on a hard disc drive. Previous studies have not considered the effects of space and physical size on these networks, as space has little effect on the network physical configuration.

Other infrastructure networks, on the other hand, such as electrical transmission networks or transportation networks, require large amounts of space and are usually subject to strict planning regulations. A few studies have considered the spatial configuration of real-world networks, such as airline networks (for example, Guimera and Amaral 2004; Burghouwt et al. 2003; Qian and Han 2009; Gastner and Newman 2006); however, these studies have not considered hazard tolerance.

The 2010 eruption of the Eyjafjallajökull volcano, in Iceland, occurred on the 14th March forcing almost 800 local residents to evacuate their homes (Petersen 2010). With further eruptions, airspace in Europe became restricted, and no fly zones came into operation on 14th April (Brooker 2010) (see Fig. 2a–c). The resulting airport closures and disruption to air travel caused more than 10 million passengers to be delayed. The economic impact to the airline industry, in terms of revenue loss for airlines from scheduled services, during the period 15th–21st April, was estimated at 1.7 billion US dollars (Mazzocchi et al. 2010). We show that this disruption was disproportionate by quantifying the magnitude of the disturbance relative to the cause. We have achieved this using the data contained in Openflights (2010) to produce a comprehensive set of 525 European airports, 3,886 air routes operated by 203 airlines as well as travel statistics for Europe for the 14th–21st April 2010 (Eurocontrol 2010). We have used these data to form a European air traffic network (EATN) and have then obtained its degree distribution, which gives us information about its inherent tolerance to random hazard. We have also investigated the tolerance of the EATN to two types of spatially coherent hazard, in both cases, taking note of the number of airports closed, air routes cancelled, the proportion of closed airspace and the maximum cluster size of the network. We have used these data to determine whether the EATN is vulnerable to spatial hazards.

2 Initial assessment of the hazard tolerance of the European air traffic network

Our first investigation into the EATN is achieved by plotting the network's degree distribution. As this is defined as the probability distribution of the number of connections that each node has to other nodes, it is therefore a key indicator of its hazard tolerance. Comparing the degree distribution of EATN (Fig. 3a) to other published research, we find that the European data set is similar to the North American (Guimera and Amaral 2004; Chi et al. 2003; Li et al. 2006) and Chinese (Li and Cai 2004) air traffic networks in that they conform to a truncated power law (Guimera and Amaral 2004). This type of network should therefore have relatively high hazard tolerance to random events.

To investigate whether the volcanic eruption had a disproportionate effect on the network, we have identified airports that had no flights for 12 or more hours on a particular day using the data of Eurocontrol (2010). We have taken these data and plotted Fig. 2a–c, showing the open and closed flight information regions (FIR), for the worst affected day of the hazard (18th April) and two other affected days. The figure shows that the ash cloud mainly affected northern Europe, but also closed central Europe on the worst day of the event. In Fig. 2d, we plot the proportion of air routes closed against the proportion of closed airspace. If the effect is proportionate to the cause (i.e. the disruption is proportionate to the area of closed airspace), then the points (representing different days of disruption and therefore different airport closures) should sit on the 45° line in the graph. From Fig. 2d, we can see that the relationship shows that the disruption was proportionally greater than the closed airspace, demonstrating the EATN is vulnerable to spatial hazards.

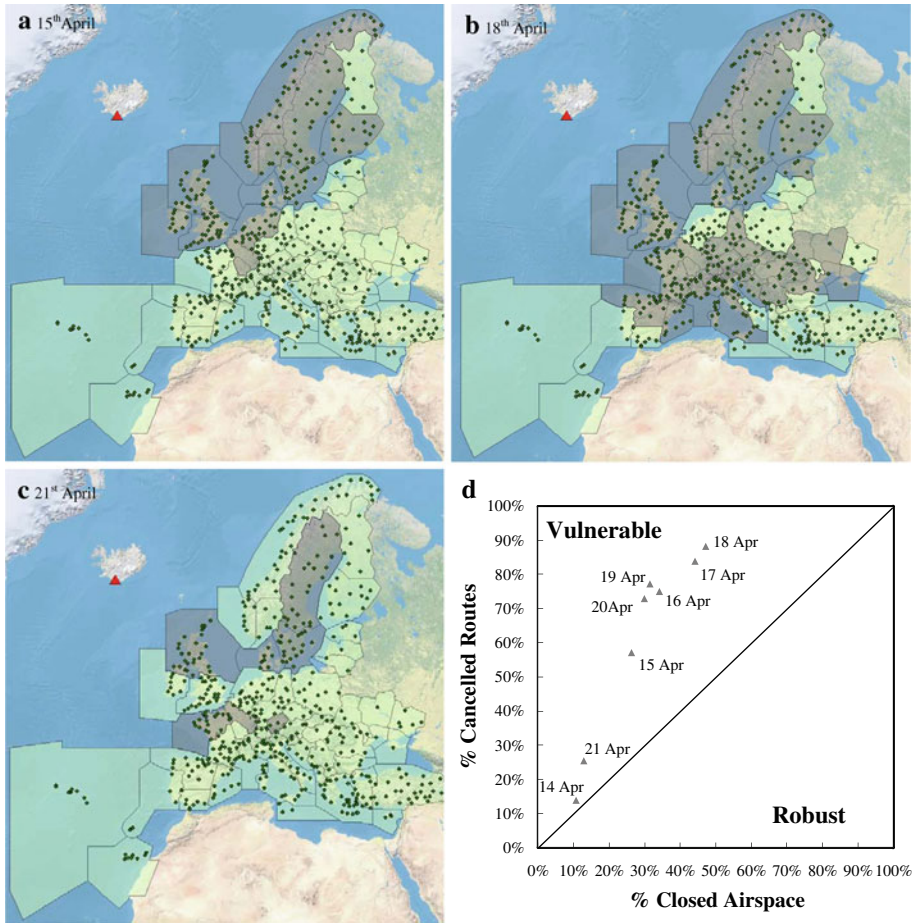


Fig. 2 Open (light green) and closed (grey) FIR in Europe (i.e. airspace) for **a** 15th April, **b** 18th April and **c** 21st April 2010 (Eurocontrol 2010). Also, **d** showing proportion of travel disruption, relative to the proportion of closed airspace, during the Eyjafjallajökull eruption of 14th–21st April 2010. The red triangle is the Eyjafjallajökull volcano

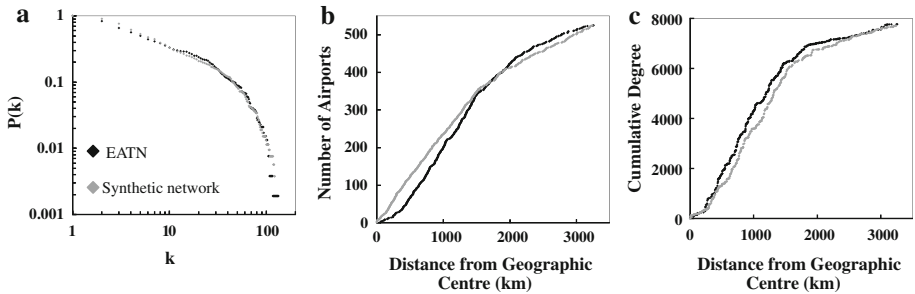


Fig. 3 **a** Cumulative degree distribution, **b** number of airports within a given radius and **c** spatial degree distribution for the EATN (data were obtained from Openflights 2010), and one generated synthetic network

To understand the influence of geography on the spatial vulnerability of the EATN, we examine the spatial distribution of European airports as well their spatial degree distribution (Fig. 3b, c). These distributions were obtained by first calculating the geographical centre of the airports (weighted by their degree) and then plotting the number of airports within a given radius (Fig. 3b) and the cumulative degree (Fig. 3c). For the EATN, the geographical centre of the network is located in Germany (approximately 190 km east of Frankfurt). Both exhibit a bilinear form, meaning that they are uniform with distance from the geographical centre of the air traffic network up to radius of $\sim 1,500$ km, after which the distribution of both airports and their degrees becomes sparser but remains relatively uniform. The change in grade shown in Fig. 3b, c occurs as the considered area extends into the Atlantic Ocean in the west, and the border of the European Union in the east.

3 Synthetic network generation algorithm

To assess the vulnerability of this class of network (not just the EATN), we have developed a synthetic network generation algorithm that not only reproduces the relational architecture of these networks but also incorporates a spatial element. In this algorithm, we propose that poorly connected nodes can capitalise on their close proximity to a highly connected hub by attracting links that were bound for the high degree hub. For example, an airline may wish to establish a route to a major regional airport; however, the operating costs at this airport are high. Flying to a nearby airport will still attract passengers as it is only a short overland journey from this node to the highly connected hub, but for this subordinate node, the fares can be reduced due to the lower operating costs. We therefore argue that the decision of where to establish a new route is made based on both degree and proximity. We use this proposition to extend the algorithm of Barabasi and Albert (1999) (used to generate scale-free networks) by enclosing the network within a spatial domain and preferentially attaching new nodes based on the degree of all nodes within a sub-domain (neighbourhood) (Fig. 1c, d). Following Barabasi and Albert (1999), we initially choose a given number of starting nodes, m_0 , but each starting node is now given a random location. At each step, we add a new node to the network and assign it a random distance bearing from the geographical centre so that the spatial distribution has the same form as shown in Fig. 3b. We then generate, between 1 and m_0 , links and preferentially attach this node to the existing network in the same manner as for a scale-free network; however, preference is now based on the degree of all nodes within the neighbourhood of the node we are attempting to attach to. The size of the neighbourhood is set by assigning a radius, r , which represents the distance people are prepared to travel overland to reach an airport. Setting the radius to zero removes the spatial dependence of the network resulting in a scale-free network, while setting the radius to twice the size of the spatial domain results in random attachment. To obtain the same spatial degree distribution as EATN, the radius of an airport's neighbourhood is made proportional to the distance the airport is from the centre of the network giving people a greater selection of routes for smaller overland travel distances.

Our new algorithm also includes the modification of Guimera and Amaral (2004), which allows a proportion of the new links, p , to connect to pre-existing nodes. This simulates the establishment of new routes between existing airports and is necessary to reproduce re-configurable networks, such as the EATN. We do not include the flight distance criteria for preferential attachment of Guimera and Amaral (2004), as we are not considering

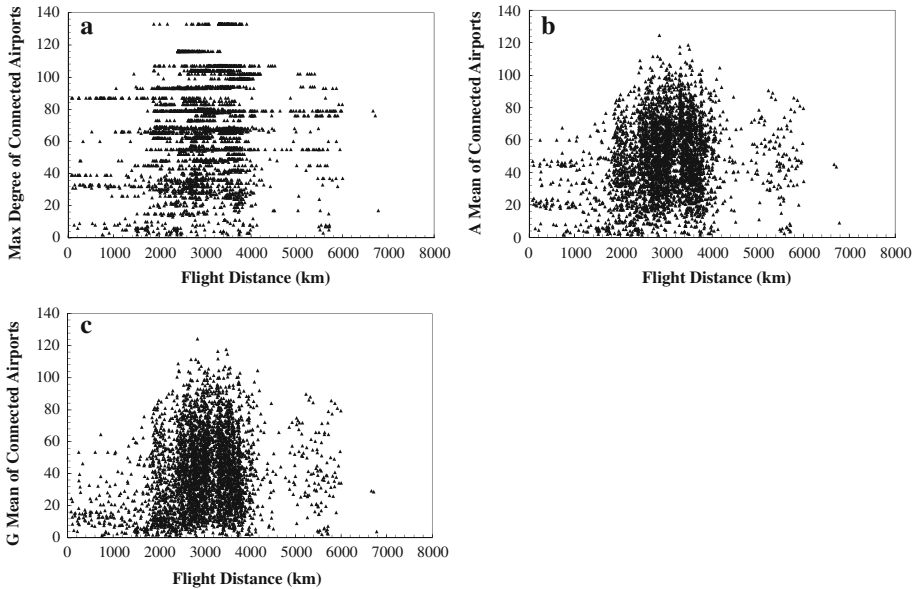


Fig. 4 The air route distance between airports (in km) compared to **a** maximum degree of connected airports, **b** arithmetic mean of the two connected airports and **c** geometric mean of the two connected airports for the EATN. All of the graphs in the figure show that there is no correlation between the air route distance (i.e. the distance between two airports connected via an air route) and various measures of degree of the two connected airports

intercontinental flights and deregulation of the EATN has led to flight path length becoming uncorrelated from degree. We demonstrate this by plotting, in Fig. 4, flight length of different air routes against various measures of degree, showing that there is no correlation between the flight length and connectivity of an airport. In Fig. 4a, we compare the maximum degree airport that an air route is connected to; in Fig. 4b, we compare the arithmetic mean of the degree of the two airports that an air route connects; and in Fig. 4c, we compare the geometric mean of the two airports that an air route connects. These figures show that there is no correlation between degree and flight path length for the EATN.

To generate the bilinear distribution in Fig. 3b, we define a distance from the geographical centre inside which a percentage of the total nodes in the network are randomly placed, with the remainder of the nodes being randomly placed in the area between this point and the outer edge of the network. This results in the number of airports within a given radius being an approximation of the EATN.

We demonstrate this algorithm by generating a 525-node synthetic network with $m_0 = 14$, $r = 0.15$ (an average distance of approximately 250 km around 2–3 h driving time on modern roads) and $p = 0.8$. The resultant degree and spatial degree distributions are shown in Fig. 3 and fit our European data set extremely well.

To demonstrate that our algorithm best fits the data over the entire distribution, we vary these parameters to gauge their influence on the degree distribution (Fig. 5). The best fit for the EATN is the exponential network with $p = 0.8$ and $r = 0.15$. Generating networks with $p = 0$ and $r = 0.15$ shows that the distribution is exponential (i.e. it is linear when

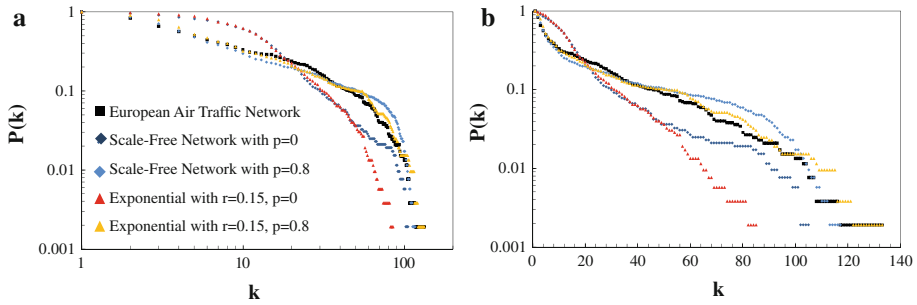


Fig. 5 EATN and four synthetic networks, generated using different algorithms, showing **a** degree distribution plotted on log–log scales and **b** degree distribution plotted on log-linear scales, where p is the proportion of new links, introduced in each time step that are allowed to connect to pre-existing nodes (e.g. if $p = 0.8$ then 80% of the new links will be between existing nodes), and r is the neighbourhood size, representing the distance that people are prepared to travel overland to an airport (e.g. if $r = 0.15$, then the equivalent distance is approximately 250 km)

plotted on log-linear axes). The difference between the exponential networks with values of $p = 0$ and $p = 0.8$, for the same value of r , demonstrates that in generating airline networks, new links will form between two existing nodes for a given time step (i.e. new flight routes will be added by an airline between existing airports) and are not only confined to attaching between the new node and existing nodes (see Guimera and Amaral 2004). If new routes are not permitted to form between existing airports (i.e. $p = 0$), the resultant is fewer ‘hub’ airports forming (i.e. airports with large degrees). Both scale-free networks follow the initial curve of the EATN data, but then do not follow the truncated part of the network, meaning that our synthetic exponential network generation algorithm produces the best fit for the EATN.

In reproducing the EATN, the r value used suggests that, on average, air passengers are prepared to travel approximately 250 km overland to an airport. In a disaster scenario, this value is unlikely to remain constant. Air passengers are likely to be prepared to take much greater overland journeys to ensure that they reach their destinations, especially in the case of returning journeys. In fact, during the Eyjafjallajökull event, accounts of people driving across Europe were not uncommon. While air transport regulations do allow for a spontaneous change of destination in hazardous situations, air space regulations, as well as airline-specific infrastructure problems, make it extremely difficult to quickly open alternative routes. In this sense, the network is more complex and rather inflexible in comparison with other networks, such as the Internet. For example, a flight en route from Zurich to Manchester may get permission for an emergency landing, at say Heathrow. If Manchester airport was closed for several days and Heathrow airport remained open, passengers may take the option of travelling to and from Heathrow to Manchester. The redirection of air traffic and the increased overland journeys that people may be prepared to make have not been taken into account in this analysis due to their unpredictability.

4 Assessment of hazard tolerance of this generic class of network

To better assess the vulnerability of this class of network and the associated scatter between different networks, we use our algorithm to generate three synthetic networks, with the same spatial properties and the same network architecture as the EATN (but each

with different node positions and linkages), and expose them to different spatial hazards. To simulate the Eyjafjallajökull event, we place a circular hazard at the edge of our domain and gradually increase its size, removing links and nodes as they become enveloped by this hazard. We also expose these networks to random but spatially coherent hazards, defined by a circle of varying diameters and random locations. To enable equivalent comparisons, the spatial hazards, for both the EATN and our synthetic networks, cover the same percentage airspace and are located at the same distance from their geographical centres. The results of these simulations are displayed in Fig. 6a, b, together with the Eyjafjallajökull event and the EATN exposed to our random, spatially coherent hazard. The scatter in the hazard tolerance for these synthetic networks is surprisingly small and is in good agreement with the EATN, demonstrating this class of network’s vulnerability to both hazards. Although the individual hazard tolerance results of our synthetic networks compare very favourably with the EATN, there are a few outliers, for example, there are two points in Fig. 6a, relating to the EATN subjected to random hazard that occurs below the 45° line. These two random hazards occur in northern Scandinavia, where both the density of airports and the average degree of airports are lower than that for central Europe, due to this region being in close proximity to the edge of the spatial boundary of the network. This results in flights from northern Scandinavia only being permitted to travel to airports with a more southerly location (i.e. stay within the boundaries of European airspace), resulting in airports with disproportionately low degrees. This results in fewer cancelled air routes for the same number of closed airports.

For our final investigation into hazard tolerance, we plot the maximum cluster size (MCS) in Fig. 6c, d. This last measure is defined as the ratio of the largest connected

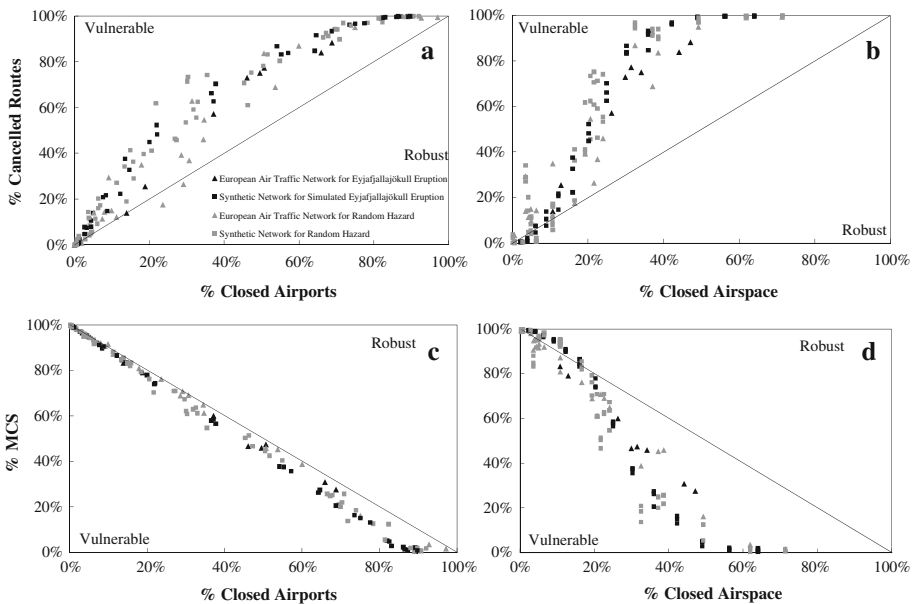


Fig. 6 Comparison of network vulnerability for the EATN and our three synthetic networks, showing **a** the impact of airport closure on air route operations; **b** the influence of airspace closure on air route operations; **c** the reduction in MCS due to airport closures; and **d** the influence of airspace closure on MCS

cluster in a fragmented network to the original size of network and therefore is a key indicator of how degraded a network has become (see Albert et al. 2000 for further details). In Fig. 6, we see that, as expected, the MCS versus proportion of closed airports for the EATN and our three synthetic networks falls on the neutral line (Albert et al. 2000); however, as our simulations and the real EATN show, it is vulnerable when measured as a proportion of closed airspace. Both our algorithm and the data show that these networks usually have neutral tolerance to spatial hazard up to about 10–15%, of the total network area, but become increasingly vulnerable after this. In the case of random hazard, both our algorithm and the EATN data set demonstrate that it is possible for a relatively small spatially coherent hazard to have a devastating effect on this class of network. This is best demonstrated in Fig. 6d, where two points on our synthetic network are centred over the geographical centre of the network resulting in a devastating effect.

5 Conclusion

In summary, the eruption of Eyjafjallajökull in 2010 caused a massive disruption to the European air traffic network. We have demonstrated that the effect on air traffic was disproportionately severe due to the network possessing a truncated, scale-free distribution and a spatial degree distribution that is uniform with distance from the centre of the network, resulting in a network that is vulnerable to spatial hazards. We believe that these distributions result from a combination of the desirability of a location, space limitations and the distance users are prepared to travel overland to an airport. As many real-world networks have been shown to be either scale free or exponential (Albert et al. 2004; Crucitti et al. 2004), it is possible that the underlying growth rules for these types of networks may result in them also being susceptible to spatial hazard. In the future, it may be desirable to reduce this susceptibility to spatial hazard. One possible method is to move some of the airports away from the geographical centre, located in Germany (specifically the high-degree airports); however, this approach may render the network less effective for normal operations. This approach also encounters the problem that each country in Europe may desire a ‘hub’ airport, meaning that moving airports away from the geographical centre may not be a possibility. Another method could be to enable reconfiguration of air routes for cases such as the Eyjafjallajökull eruption.

Acknowledgments The flight information regions necessary to define the closed airports was provided by EUROCONTROL. GIS advice on handling the data sets was provided by Dave Alderson and Ali Ford of Newcastle University. Maximum cluster size was calculated using Network Workbench. This research was partly funded by the Engineering and Physical Sciences Research Council, UK, and their support is gratefully acknowledged.

Open Access This article is distributed under the terms of the Creative Commons Attribution Noncommercial License which permits any noncommercial use, distribution, and reproduction in any medium, provided the original author(s) and source are credited.

References

- Albert R, Jeong H, Barabasi AL (1999) Internet—diameter of the world-wide web. *Nature* 401(6749):130–131
- Albert R, Jeong H, Barabasi AL (2000) Error and attack tolerance of complex networks. *Nature* 406(6794):378–382

- Albert R, Albert I, Nakarado GL (2004) Structural vulnerability of the North American power grid. *Phys Rev E* 69. doi:[10.1103/PhysRevE.69.025103](https://doi.org/10.1103/PhysRevE.69.025103)
- Barabasi AL, Albert R (1999) Emergence of scaling in random networks. *Science* 286(5439):509–512
- Barabasi AL, Oltvai ZN (2004) Network biology: understanding the cell's functional organization. *Nat Rev Genet* 5(2):101–113
- Brooker P (2010) Fear in a handful of dust: aviation and the Icelandic volcano. *Significance* 3:112–115
- Burghouwt G, Hakfoort J, van Eck JR (2003) The spatial configuration of airline networks in Europe. *J Air Transp Manag* 9(5):309–323. doi:[10.1016/s0969-6997\(03\)00039-5](https://doi.org/10.1016/s0969-6997(03)00039-5)
- Chi LP, Wang R, Su H, Xu XP, Zhao JS, Li W, Cai X (2003) Structural properties of US flight network. *Chin Phys Lett* 20(8):1393–1396
- Crucitti P, Latora V, Marchiori M (2004) A topological analysis of the Italian electric power grid. *Physica A Stat Mech Appl* 338(1–2):92–97. doi:[10.1016/j.physa.2004.02.029](https://doi.org/10.1016/j.physa.2004.02.029)
- Eurocontrol (2010) Monthly network operations report: April 2010
- Gastner MT, Newman MEJ (2006) The spatial structure of networks. *Eur Phys J B* 49(2):247–252. doi:[10.1140/epjb/e2006-00046-8](https://doi.org/10.1140/epjb/e2006-00046-8)
- Guimera R, Amaral LAN (2004) Modeling the world-wide airport network. *Eur Phys J B* 38(2):381–385. doi:[10.1140/epjb/e2004-00131-0](https://doi.org/10.1140/epjb/e2004-00131-0)
- Li W, Cai X (2004) Statistical analysis of airport network of China. *Phys Rev E Stat Nonlin Soft Matter Phys* 69(4 Pt 2):046106
- Li W, Wang QA, Nivanen L, Le Mehaute A (2006) How to fit the degree distribution of the air network? *Physica A Stat Mech Appl* 368(1):262–272. doi:[10.1016/j.physa.2005.11.050](https://doi.org/10.1016/j.physa.2005.11.050)
- Mazzocchi M, Hansstein F, Ragona M (2010) The 2010 volcanic ash cloud and its financial impact on the European airline industry. *CESifo Forum* 11:92–100
- Openflights (2010) OpenFlights.org. <http://openflights.org/>. Accessed 13 Aug 2010
- Oroian I (2010) Eyjafjallajökull volcano eruption—a brief approach. *ProEnvironment* 3:5–8
- Petersen GN (2010) A short meteorological overview of the Eyjafjallajökull eruption 14 April–23 May 2010. *Weather* 65(8):203–207. doi:[10.1002/wea.634](https://doi.org/10.1002/wea.634)
- Qian JH, Han DD (2009) A spatial weighted network model based on optimal expected traffic. *Physica A Stat Mech Appl* 388(19):4248–4258. doi:[10.1016/j.physa.2009.05.047](https://doi.org/10.1016/j.physa.2009.05.047)
- Strogatz SH (2001) Exploring complex networks. *Nature* 410(6825):268–276